

Journal Pre-proofs

Synthesis, Structure, Polyphenol Oxidase Mimicking and Bactericidal Activity of a Zinc-Schiff Base Complex

Shreya Mahato, Nishith Meheta, K Muddukrishnaiah, Mayank Joshi, Madhusudan Shit, Angshuman Roy Choudhury, Bhaskar Biswas

PII: S0277-5387(20)30590-8
DOI: <https://doi.org/10.1016/j.poly.2020.114933>
Reference: POLY 114933

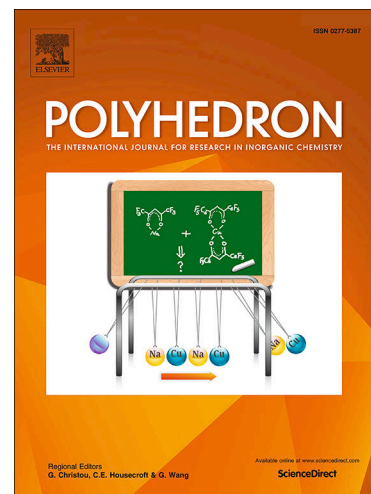
To appear in: *Polyhedron*

Received Date: 9 September 2020
Accepted Date: 18 November 2020

Please cite this article as: S. Mahato, N. Meheta, K. Muddukrishnaiah, M. Joshi, M. Shit, A. Roy Choudhury, B. Biswas, Synthesis, Structure, Polyphenol Oxidase Mimicking and Bactericidal Activity of a Zinc-Schiff Base Complex, *Polyhedron* (2020), doi: <https://doi.org/10.1016/j.poly.2020.114933>

This is a PDF file of an article that has undergone enhancements after acceptance, such as the addition of a cover page and metadata, and formatting for readability, but it is not yet the definitive version of record. This version will undergo additional copyediting, typesetting and review before it is published in its final form, but we are providing this version to give early visibility of the article. Please note that, during the production process, errors may be discovered which could affect the content, and all legal disclaimers that apply to the journal pertain.

© 2020 Published by Elsevier Ltd.



Synthesis, Structure, Polyphenol Oxidase Mimicking and Bactericidal Activity of a Zinc-Schiff Base Complex

Shreya Mahato,^a Nishith Meheta,^a K Muddukrishnaiah,^b Mayank Joshi,^c Madhusudan Shit,^d Angshuman Roy Choudhury,^c and Bhaskar Biswas^{a,*}

^aDepartment of Chemistry, University of North Bengal, Darjeeling-734013, India

^bDepartment of Pharmaceutical Technology, Anna University, BIT Campus Thiruchirappalli, India

^cDepartment of Chemical Sciences, Indian Institute of Science Education and Research, Mohali, Sector 81, Knowledge City, S. A. S. Nagar, Manauli PO, Mohali, Punjab 140306, India

^dDepartment of Chemistry, Dinabandhu Andrews College, Kolkata 700084, India

Focusing on the important biological functions of metallo-enzymes and metallo-therapeutics in living world, this research work demonstrates the synthesis, crystal structure, supramolecular architecture, 4-methylcatechol oxidation and bactericidal activity of an interesting zinc-Schiff base complex, $[\text{Zn}(\text{HL})_2\text{Cl}_2]$ (**1**), [Schiff base (HL) = 2-(2-methoxybenzylideneamino)phenol]. Crystal structure analysis of the zinc-Schiff base reveals that zinc centre exists in a distorted tetrahedral geometry. The Schiff base adopts three donor centres, however it gets protonated to exist in a zwitter ionic form and behaves as a monodentate coordinator in **1**. This zinc-Schiff base complex has been examined towards the bio-mimetic oxidation of 4-methylcatechol (4-MC) in methanol and portrays its good efficacy with good turnover number, $1.45 \times 10^3 \text{ h}^{-1}$. Electro-chemical study, electron paramagnetic resonance analysis and electrospray ionization mass spectrometry results for the zinc-Schiff base complex in presence of 4-MC ensures that the catalytic reaction undergoes through enzyme-substrate binding, and generation of radical in the course of catalysis drives the catalytic oxidation of 4-MC. Antibacterial study has also been performed against few clinical pathogens (*Bacillus* SP, *Enterococcus*, and *E.coli*). Scanning electron microscope and EDAX analysis for the pathogen with little dose of zinc complex confirms the destruction of bacterial cell membrane with 1.44% occurrence of zinc in the selected zone of inhibition area. This observation holds a great promise to develop future antibacterial agent.

Keywords: Zinc(II); Electrochemical analysis; 4-methylcatechol oxidation; Schiff base; X-ray structure; Bactericidal activity

*Corresponding author. E-mail: bhaskarbiswas@nbu.ac.in / icbbiswas@gmail.com

1. Introduction

In the field of coordination chemistry, Schiff base, a unique class of compounds has been emerged as a widely used chelator towards the development of metal complexes [1-7]. The newly prepared Schiff bases and their coordination compounds hold a great promise to scientific community for their novel properties in designing efficient catalysts, smart magnetic materials, important therapeutics, opto-electronic devices, bio-mimetic models and so on [8-14]. Among the different 3d elements, zinc is an indispensable bio-metal in living system which has significant **functions** in various biological processes [15]. Most captivatingly, zinc-Schiff-base complexes have been well recognized for their catalytic, opto-electronic and therapeutic properties [13,14,16-21]. Zinc ion in association with Schiff base exhibits diversified coordination geometries [22,23] **and interesting** supramolecular architectures [24]. Added to this, zinc-Schiff base complexes also provide promising potency towards the resistance of microbial activity and consider as **one of the** suitable candidates for the discovery of potent metallo-therapeutics [25-27].

Polyphenol oxidase (PPO) consists of a group of copper containing proteins which monitors the browning of wide range of natural fruits, vegetables, and sea-food products through the enzymatic oxidation of phenolics and lead to the development of brown pigments [28,29]. PPO catalyzes the hydroxylation of monophenol (monophenolase activity) following the subsequent oxidation of diphenol to quinones (diphenolase activity) which promptly convert to brown coloured relatively insoluble polymers (melanins) [30]. This development of brown colour catalyzed by PPO has received paramount attention in food industry as it provides significant information about nutritional quality and, thereby, produced a crucial economic impact on the food-processing industry [31]. Scientific literatures exhibit that the rate of metallo-enzyme catalysed browning of natural fruits as well as vegetables fundamentally depends on concentrations of phenolic substrate, pH, temperature, and specific activity of the PPO [28-31]. It is also well documented that catalytic oxidation of phenols actually produces biologically important *o*-quinones which exhibits facile redox reactions for its higher chemical activity. The *o*-quinone also plays various biological functions likely to

develop antibiotics, defensive secretions, and pigmentation [32]. Melanin pigment, a polymerise form of *o*-quinone protects all the living organisms from UV-light of sun [33]. In the context, with an aim to study the bactericidal activity and catalytic fate towards the bio-mimetic oxidation of 4-MC, we have designed, synthesized, and structurally characterized of an interesting zinc-Schiff base complex and studied its bactericidal and bio-mimicking activity.

2. Experimental

2.1. Preparation of the Schiff base and zinc-Schiff base complex

(a) Chemicals, solvents and starting materials

Highly pure *o*-anisidine (Sigma Aldrich, USA), salicylaldehyde (Sigma Aldrich, USA) and zinc chloride hexahydrate (Merck, India) were purchased from the respective outlets. All the chemicals and solvents were of analytical grade and used as received without further purification.

(b) Synthesis of the Schiff base and zinc-Schiff base complex

The synthetic details and spectroscopic characterization of this Schiff base, HL was recently reported by our group [34].

The zinc-Schiff base complex was synthesized by addition of solid zinc(II) chloride hexahydrate (0.244 g, 1 mmol) to aqueous-methanolic solution of HL (0.454 g, 2 mmol). The yellow coloured solution of Schiff base was turned to bright yellow solution. After that, the reaction mixture was kept for slow stirring for ~30 mins and set in open atmosphere for slow evaporation. Bright yellow coloured single crystals of zinc-Schiff base were separated out after 10-12 days. The crystalline compound was washed with hexane and dried over silica gel. Finally, different spectroscopic methods were employed to establish the molecular composition of zinc-Schiff base and the results are summarized as follows.

Yield of **1**: 0.415 g (~63.5% based on metal salt) Anal. Calc. for $C_{28}H_{26}N_2O_4Zn$ (**1**): C, 56.92; H, 4.44; N, 4.74; Found: C, 56.95; H, 4.41; N, 4.80. IR (KBr pellet, cm^{-1} ; Fig. S1): 3571, 3488 ($\nu_{C=N}$), 1623, 1609 ($\nu_{C=N}$); UV-Vis (1×10^{-4} M, $\lambda_{max}(abs)$, nm, MeOH; Fig. S2): 230, 269, 344; 1H NMR (δ ppm, 400 Mz, DMSO- d_6 ; Fig. S3) δ = 13.79 (s, 2H), 8.94 (s, 2H), 7.41-6.92 (Ar-H, 16H), 3.84 (t, 6H) ppm. ^{13}C NMR (400 MHz, DMSO- d_6 ; Fig. S4): 192.26 (HC=NH $^+$), 163.03, 161.22 (HC=N), 153.09 (Ar-N=C), 136.81, 133.54, 132.90, 129.74, 128.65, 119.81,

119.64, 117.68, 117.16, 114.53, 114.53, 112.68 (Ar-C), 56.23, 55.66 (-OCH₃). ESI-MS (m/z, MeOH; Fig. S5): [Zn(HL)(CH₃OH)₂+H], 310.14 (Theoretical m/z 310.10).

2.2. Physical measurements

FT-IR spectra of the Schiff base and zinc-Schiff base were recorded with a FTIR-8400S SHIMADZU spectrophotometer (Shimadzu, Kyoto, Japan) from 400 to 3600 cm⁻¹ with KBr pellet. ¹H and ¹³C NMR spectra of the Schiff base ligand (HL) were measured on a Bruker Advance 400 MHz spectrometer (Bruker, Massachusetts, USA) in CDCl₃ at 298 K. Steady-state absorption and other electronic bands were recorded with a JASCO V-730 UV-Vis spectrophotometer (Jasco, Tokyo, Japan). Electrospray ionization (ESI) mass spectrum zinc-Schiff base was recorded using a Q-tof-micro quadrupole mass spectrometer. Elemental analyses were performed on a Perkin Elmer 2400 CHN microanalyser (Perkin Elmer, Waltham, USA). X-band EPR spectrum was recorded with a Magnettech GmbH MiniScope MS400 spectrometer (equipped with temperature controller TC H03, Magnettech, Berlin, Germany).

2.3. Crystal structure determination and refinement

A Rigaku XtaLABmini diffractometer equipped with Mercury 375R (2×2 bin mode) CCD detector was employed to collect the X-ray diffraction data for zinc-Schiff base. The data were collected with graphite monochromated Mo-K α radiation ($\lambda=0.71073$ Å) at 298 K using ω scans. The data were reduced using CrysAlisPro 1.171.39.35c [35] and the space group determination was done using Olex2. The structure was resolved by dual space method using SHELXT-2015 [36] and refined by full-matrix least-squares procedures using the SHELXL-2015 [37] software package through OLEX2 suite [38]. All hydrogen atoms were geometrically fixed.

2.4. Hirshfeld surface analysis of zinc-Schiff base complex

Hirshfeld surfaces and 2D fingerprint plots for the zinc-Schiff base complex were generated employing Crystal Explorer 17.5 [39] program to understand the involvement of intermolecular interactions in crystal packing. The function, d_{norm} is used to find out the ratio of the distances of any surface point to the nearest interior (d_i) and exterior (d_e) atom and the

van der Waals radii of the atoms [40,41]. The normalized contact distance (d_{norm}) is expressed as

$$d_{norm} = \frac{d_i - r_i^{vdw}}{r_i^{vdw}} + \frac{d_e - r_e^{vdw}}{r_e^{vdw}} \quad \dots(1)$$

Where, r_e^{vdw} and r_i^{vdw} denote the corresponding van der Waals radii of atoms. The details of analysis can be obtained elsewhere [39-41].

2.5. 4-methylcatechol oxidation study

The oxidation of 4-methylcatechol (4-MC) was carried out by addition of 1×10^{-4} M solution of zinc complex with 1×10^{-2} M of 4-MC solution in methanol. The course of catalysis was performed under aerobic conditions. The wavelength scans of catalytic oxidation were monitored through a UV-Vis spectrophotometer with an interval of 8 minutes for 2h from 200-700 nm [10,11,17-20,42-44].

Kinetic experiments were performed with a spectrophotometer and kinetic parameters were analysed to understand the course of 4-MC oxidation by this zinc-Schiff base in MeOH [17-20]. 0.04 mL 1×10^{-4} M of zinc-Schiff base solution was treated with 2 mL of 4-MC with a variation of its concentration from 1×10^{-3} M to 1×10^{-2} M in order to achieve the final concentration of zinc-Schiff base as 1×10^{-4} M. The catalytic conversion of 4-MC was monitored with the progress of time at 409 nm (time scan) in MeOH [42-46]. All the kinetic experiments were performed in triplicate.

The extraction of purified oxidation product of PPO has remained difficult because of irreversible binding of high phenolic content in purification steps. Different scientists showed different way of extraction for catechol oxidation product, o-quinone. Suyama and group [45] extracted the oxidation product of 4-MC as 4-methyl-o-quinone (4MQ) in treatment with *n*-butylamine under oxygen saturated environment. In general, amines preferably attack the oxidized catechols by either Michael-type addition or through formation of a Schiff base [46]. In 2018, we were successfully isolated the single crystals of 3,5-di-*tert*-butyl-o-quinone in association with the hydrogen bonded catechol in non-aqueous medium [14]. In this 4-MC oxidation, the red coloured product was isolated employing column chromatography with *n*-hexane-diethyl ether solvent mixture (9:1, v/v). The **identification** of the product was **confirmed** by a comparison of spectral data between the extracted compound and reported

compound. ^1H NMR data for 4-methyl-*o*-quinone, (CDCl_3 , 400 MHz,) δ_{H} : 6.76 (m, 1H), 6.64 (d, 1H), 6.52 (d, 1H), 2.18 (s, 3H).

2.6. Electro-chemical analysis

BASi Epsilon-EC was employed to carry out the for cyclic voltammetric experiments in CH_2Cl_2 solutions containing 0.2 M tetrabutylammonium hexafluorophosphate as supporting electrolyte. The BASi platinum working electrode, platinum auxiliary electrode, Ag/AgCl reference electrode were used for the measurements.

2.7. Clinical bacterial cultures and culture media

The antimicrobial property of the zinc-Schiff base was examined against few clinical pathogenic bacteria like *Bacillus* SP, *Enterococcus* and *E. coli*. Clinical Microbial cultures were procured from government medical college from Tiruchirappalli, Tamil Nadu. Muller-Hinton agar media of Himedia Pvt. Bombay, India was used for the media for the microbial test. The antibacterial activity was evaluated by using the Himedia zone reader.

2.7.1. Inoculums preparation

The collected clinical pathogens, *Bacillus* SP, *Enterococcus* and *E.coli* were inoculated individually in 5 mL of sterile nutrient broth (NB) media and incubated at 37°C for 24h. Thereafter, 200 μL of the fresh culture of organisms was dispensed into 30 mL sterile nutrient broth and incubated 24 h to standardize the bacterial culture to 10^8 CFU/ml (colony forming units).

2.7.2. Agar well diffusion method (Kirby-Bauer method)

The bactericidal activity of the synthesized zinc-Schiff base compound and a standard marketed drug (Amikacin, 100 mg/2mL) was studied initially by using agar well plate method [47]. *Bacillus* SP, *Enterococcus* and *E.coli* inoculums were prepared by using sterile nutrient broth media. Mueller Hinton agar double strength media were made by autoclaving 760 mg in 100 mL. Standardized inoculums inoculate the test microorganisms on the Mueller Hinton agar plates by using sterile cotton swabs. Four 8 mm diameter agar wells were prepared using sterile cork-borer, and 100 μL (50 mg/mL) zinc-Schiff base complex and Amikacin 5 μL (10 mg/mL) were placed on agar well using micropipette under aseptic conditions. Sterile water used as a negative control. Agar plates were incubated for 30 min in the refrigerator to diffuse the formulation into the agar, and finally, plates were incubated at 37°C for 24 h. Antibacterial activity was evaluated by using the Himedia zone reader.

Preparation of stock solutions for MIC

Weight of the powder (mg) =

$$\frac{\text{Volume of solution (mL)} \times \text{Concentration (mg/L)}}{\text{The potency of powder (mg/g)}}$$

2.7.3 Determination of MIC and MBC for zinc-Schiff base against clinical bacillus SP

The method of micro-dilution was used to establish the antibacterial potential of the zinc-Schiff base and respective controls. A spectrophotometer (OD₅₉₅ = 0.22) equivalent to 10⁸ CFU/mL was used to fix the bacterial cultures to 0.22 optical density at 595 nm. Different concentrations of zinc-Schiff base (100, 50, 25, 12.5, 6.25 mg/mL) and standard drug (50, 25, 12.5, 6.25, 3.125, 1.5625 mg/mL) were added in 2 mL MIC tubes as the respective controls. 100 µL of the zinc-Schiff base solutions were added to each MIC test tube. MIC tubes were incubated overnight at 37 °C for 24 h.

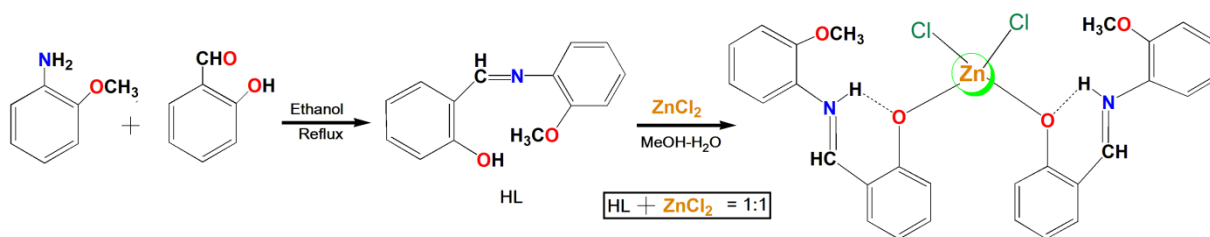
2.7.4 Antimicrobial activity of zinc-Schiff base with field emission scanning electronic microscope (FESEM) and energy dispersive X-ray analysis (EDAX)

The area showing an inhibition against the clinical *Bacillus* SP pathogen on the MHA plate was removed by cutting agar, fixed by soaking in 2 % glutaraldehyde in cacodylate buffer 0.1 M for 60 min [48]. The samples were washed with 0.1 M cacodylate buffer and added in triplicate for successive 60 min wash. Samples were placed in a freshly prepared cold cacodylate buffer for transportation into the laboratory for FE-SEM and EDAX.

3. Results and discussion

3.1. Synthesis and formulation of the Schiff base (HL) and zinc-Schiff base complex

The Schiff base was obtained from the condensation between salicylaldehyde with *o*-anisidine under reflux (Scheme 1). The synthetic route of zinc-Schiff base is presented in Scheme 1. The zinc complex was synthesized by portionwise addition of hydrated zinc(II) chloride to HL in aq.-methanol medium with slow thermal agitation on a magnetic stirrer. The mole ratio between zinc chloride and HL was varied to examine the variation in molecular composition, although the molecular formulation was determined as [Zn(HL)₂Cl₂] for every reaction. The single crystals of zinc-Schiff base were obtained employing slow evaporation technique at room temperature. The zinc complex was soluble in methanol, chloroform etc.



Scheme 1. Synthetic procedure of **1**

3.2. Description of crystal structure and Hirshfeld surface analysis of zinc complex

Crystal structure analysis reveals that the zinc-Schiff base complex crystallizes in a triclinic system with $P1$ space group. The thermal ellipsoids of the zinc complex are shown in Fig. 1. The crystal structure refinement parameter for this zinc-Schiff base complex is presented in Table 1. The metal centric bond distances and bond angles are presented in Table 2. The crystal structure of zinc-Schiff base complex looks very interesting in which two azomethine-Ns of the HL abstract two protons from phenolic-OH and lead to zwitter ionic form of the Schiff base. This phenomenon prohibits the chelation property of the Schiff base ligand and thereby HL behaves as a simple monodentate ligand instead of tridentate chelating ligand towards Zn(II) ion. The zinc centre in the crystal structure exists in distorted tetrahedral coordination geometry. The Schiff base may be considered as a zwitter ion since it contains equal number of positively- and negatively-charged functional groups. This zwitter ionic form of HL facilitates the mono-coordination of phenoxo-O to $ZnCl_2$ leading to a tetrahedral structure. Two HL units in association with two chlorides coordinate with Zn(II) ion to form tetracoordinate zinc complex. The methoxy group attached to phenyl ring in the Schiff base remains non-reactive in the complex formation. The formation of tetrahedral geometry was further evident from the values of metal centric bond angles [C11-Zn1-Cl2, 124.59(5)°; C11-Zn1-O2, 104.69(9)°; C11-Zn1-O3, 104.42(10)°; Cl2-Zn1-O2, 103.97(10)°; Cl2-Zn1-O3; 103.73(9)°; O2-Zn1-O3, 116.31(12)°]. The average bond angle value around zinc(II) centre was estimated as 109.61° which deviates little from ideal tetrahedral geometry.

Hirshfeld surface analysis of zinc-Schiff base was carried out using d_{norm} calculation with Crystal Explorer software (Fig. S6). Red highlighted areas represent d_{norm} area as well as supramolecular interactions of **1** with its neighbouring zinc complex units. The elemental contribution of each element with % share in close interaction with others is expressed in Table S1. In the d_{norm} , blue areas are showing the engagement of $\pi \cdots \pi$ interactions between

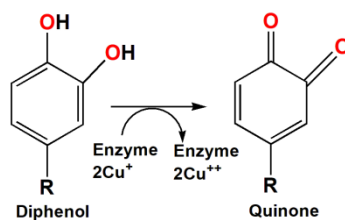
phenyl centroid of the Schiff base while red area highlights intermolecular C-H...Cl interactions and displays in Fingerprint plots (Fig. S7). Self-assembled architecture for the zinc complex displayed important C-H...Cl interactions which help to develop a 3D supramolecular structure (Fig. S8). Moreover, $\pi\cdots\pi$ interactions between the phenyl centroids of the HL provide additional strength to the 3D architecture (Fig. S9, Table S2). Previously, a crystal structure of zinc complex [ZnLCl₂] containing a different Schiff base, L = 4-methyl-2,6-di[(S)-(+)-1-phenylethylimino methyl]phenol} was reported by Das *et al.* [24]. Although we found the CIF of that structure in SI file; however we didn't find the CCDC number of the CIF in the published paper as well as in CCDC. That zinc(II) complex crystallized in orthorhombic system with $P2_12_12_1$ space group and produced supramolecular helices through C-H...Cl interaction [24]. In that case, a N,O,N type tridentate Schiff base was monoprotonated to one azomethine-N and behaves as a bidentate chelator towards Zn(II) ion. However, in our case, the Schiff base is a O,N,O-type ligand which exists in a zwitter ionic form and act as a monodentate ligand towards Zn(II) ion. The zinc complex crystallizes in triclinic system with $P1$ space group and forms a 3D architecture employing C-H...Cl and $\pi\cdots\pi$ interactions in the crystalline phase (Fig. S8, Fig. S9, Table S2). The reported value for C-H...Cl hydrogen bond by Das *et al.* [24] was larger (3.665 Å in length) than that of the value in the self-assembled architecture in our synthetic zinc complex. The values of C-H...Cl H-bonding are of comparable range with the reported values [49,50].

3.3. Solution behaviour of the zinc-Schiff base complex

The zinc-Schiff base shows good solubility in methanol (MeOH). The zinc complex exhibits characteristic electronic transitions at 230, 269 and 344 nm which are very close to the electronic transitions of the Schiff base (230, 270 and 346 nm). The electronic spectra for HL and zinc complex are displayed in Fig. S2. The electronic bands of zinc(II) complex at 230 and 269 nm are assignable to $n\rightarrow\pi^*$ and $\pi\rightarrow\pi^*$ transitions of azomethine origin [14,17-20] and the optical band at 344 nm may be attributed as intra-ligand electronic transition [17-20,51].

3.4. 4-methylcatechol oxidation study of the zinc-Schiff base complex

The catalytic oxidation of 4-methylcatechol (4-MC) was studied by addition of catalytic amount of zinc-Schiff base to 100 fold of 4-MC under aerobic atmosphere at 25°C (Scheme 2).



Scheme 2. Catalytic oxidation by polyphenol oxidase (PPO)

The changes of absorbance upon addition of zinc complex to 4-MC solution were observed with a UV–Vis spectrophotometer. The nature of spectral change in the course of catalysis was monitored for 1h with 8 min interval (Fig. 2). Upon addition of 1×10^{-4} M zinc-Schiff base solution to 1×10^{-3} M solution of 4-MC in MeOH, a new electronic band at 409 nm with a red shift of ~ 16 nm was developed. This development of the electronic band at 409 nm was a definite signature for the production of 4-methyl-*o*-benzoquinone species in solution (Fig. 2) [14,18,20,42-44]. Controlled experiment was also performed in presence of catalytic amount of HL under identical reaction set up. No significant changes of electronic bands have been observed for 2h in the course of catalysis. This phenomenon accounts on about the non-functional activity of HL in the catalytic oxidation of 4-methylcatechol.

The kinetics for the catalytic oxidation of 4-MC was studied following Michaelis–Menten model of saturation kinetics and the method of initial rates was applied to find out the kinetic parameter.

The Michaelis–Menten equation is expressed as:

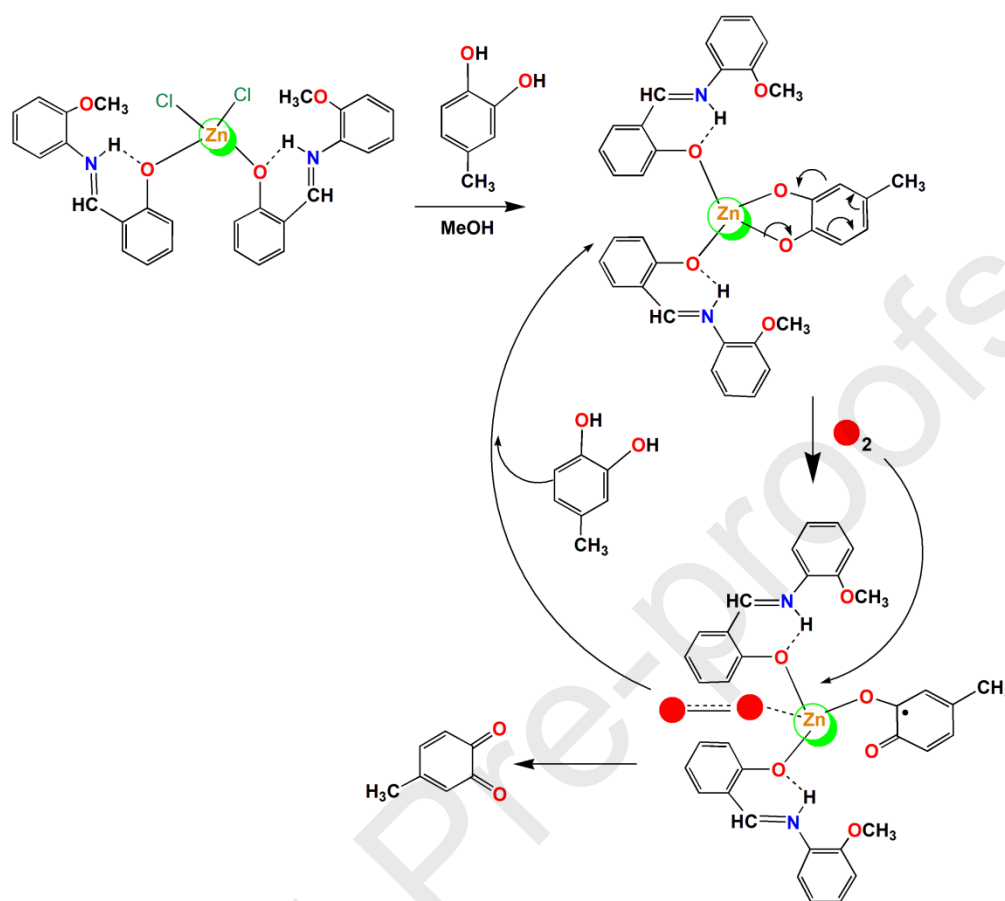
$$V = \frac{V_{max} [S]}{K_M + [S]} \dots\dots\dots(2)$$

Where, V indicates the velocity of reaction (rate of the reaction), K_m expresses the Michaelis–Menten constant, V_{max} presents the maximum reaction velocity, and $[S]$ is the substrate concentration. The growth of 4-methyl-*o*-benzoquinone species was monitored at 409 nm with the function of time [14,18,20,34,35,41]. The profile of kinetics was plotted rate constants vs. substrate concentration (Fig. S10). The values of kinetics parameters were determined as $V_{max}(\text{MS}^{-1}) = 4.03 \times 10^{-3}$; $K_M = 1.38 \times 10^{-3}$ [Std. Error for $V_{max}(\text{MS}^{-1}) = 4.81 \times 10^{-4}$; Std. Error for $K_m(\text{M}) = 5.53 \times 10^{-4}$]. A comparison of K_M values towards the oxidation of 4-MC by the zinc-Schiff base as well as in natural sources is summarized in Table 3 [52,53]. The zinc-Schiff base catalyzed the oxidation of 4-MC under aerobic atmosphere with high efficacy, $k_{cat}/K_M = 1.05 \times 10^6 \text{ h}^{-1}$.

3.5. Mechanistic studies on 4-methylcatechol oxidation

The electrochemical potentials of the zinc-Schiff base in absence and presence of 4-MC were studied with cyclic voltammetry in CH_2Cl_2 at 295 K. The redox potential data referenced to ferrocenium/ferrocene (Fc^+/Fc) couple are summarized in Table S3. The cyclic voltammograms of zinc complex and its reaction mixture with 4-MC are illustrated in Fig. 3. In the cyclic voltammogram of zinc-Schiff base, two reversible anodic peaks at 0.064 V and 0.421 V were developed for the oxidation of two phenoxide ion in two Schiff base ligands which are assignable to phenoxide/phenoxide radical ($\text{O}^-/\text{O}^{\bullet-}$) redox couple in the solution. The zinc-Schiff base didn't exhibit any cathodic peak indicating the stable +2 oxidation state of zinc ion. The electrochemical potential plots of the reaction mixture of zinc complex with 4-MC exhibits one reversible anodic wave at -0.55 V and one irreversible cathodic peak at -1.33 V. The appearance of anodic peak is due to oxidation of 4-methylcatechol to 4-methyl-*o*-benzosemiquinone ($\text{cat}/\text{sq}^{\bullet-}$) and the irreversible cathodic wave is attributed to the reduction of Zn^{2+} to Zn (Zn^{2+}/Zn). Thus, electrochemical analysis ensures the active participation of zinc-Schiff base and facilitates the oxidation process of catechol to benzo-semiquinone radical formation. Therefore, zinc complex exhibits metal mediated polyphenol oxidase activity through the radical pathway.

EPR studies were further investigated to consolidate the electrochemical observations in the course of catalytic oxidation of 4-MC in CH_2Cl_2 . To unveil the mechanistic insights, we have recorded the EPR spectrum of the zinc-Schiff base in presence of 4-MC in CH_2Cl_2 medium (Fig. 4). The EPR spectrum of zinc complex in presence of 4-MC at room temperature produced a characteristic signal for the development of organic radical at g ca 2.001 which strongly suggests that the course of catalysis was driven by generation of radical species (Fig. 4). The g value for oxidised 3,5-ditertbutylcatechol was previously reported as 2.0051 in 10^{-1} M Bu_4NPF_6 [14,54,55]. Scheme 3 presents the plausible mechanistic pathway for the course of catalytic oxidation of 4-MC.



Scheme 3. Plausible mechanism for the catalytic oxidation of 4-MC

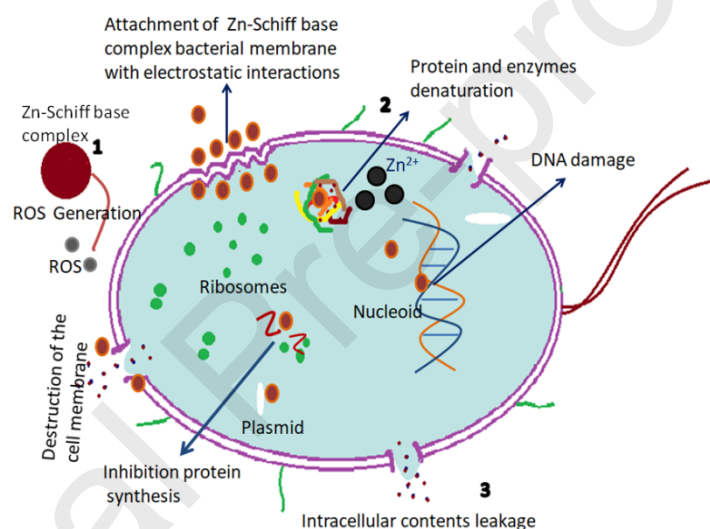
Therefore, based on the experimental outcomes of spectrophotometric titration, electrochemical analysis and electron paramagnetic measurement it may be portrayed that 4-MC initially binds with zinc-Schiff base (enzyme) complex to generate enzyme-substrate (ES) adduct with concurrent development of benzo-semiquinone radical. The zinc centre thereby supplies electron to antibonding molecular orbital of oxygen molecule to facilitate the production of *o*-benzoquinone product with returning back to ES along with the production of hydrogen peroxide. Noteworthy, if the course of 4-MC oxidation runs for longer time, there is every possibility to progress polymerisation reaction of 4-MC. To the best of our knowledge, our synthetic zinc-Schiff base complex will be the first zinc-Schiff base complex which exhibits 4-MC oxidation activity in scientific literature.

3.6. Antibacterial activity

The study of the antibacterial activity of zinc-Schiff base was initially determined by the method of well diffusion against clinical *Bacillus* SP, *Enterococcus*, and *E.coli*. The results of

the inhibition zone diameters shown in Table S4. The bactericidal efficacy of the zinc-Schiff base on *Bacillus* SP Minimum was evaluated in terms of the estimation of minimum inhibitory Concentration (MIC) and minimum bacterial concentration (MBC) (Table S5). The MIC and MBC values were obtained as 50 and 25 mg/mL respectively against *Bacillus* SP strain.

According to scientific literatures the mechanism for the destruction of cell membranes of microbial species is well established. It is experimentally proved that the generation of reactive oxygen species (ROS) remains the driving force to cause oxidative stress and leads to the damage of cell membrane and DNA. This phenomenon actually destroys microbial/bacterial species and prevents the growth of microbes effectively (Scheme 4).



Scheme 4. Zinc-Schiff base induced cell membrane destruction mechanism for *Bacillus* SP

In the context of evaluation of bactericidal activity of this zinc-Schiff base against few pathogenic bacteria, Zn²⁺ ion interacts with the enzyme, amino acids and proteins in bacteria. The specific interaction between zinc ion and cell membrane through electrostatic forces destroy the plasma membrane and cause leakage of intracellular material (Scheme 4). Herein, zinc ion prefers stronger interactions with the amino acids and proteins in bacteria and decomposition of coordination environment of the Zn(II) ion covered by two units of Schiff bases is actually occurred. Though the Schiff base contains three donor centres and should be behaved as a tridentate chelator, however in reality the Schiff base acts as a simple monodentate ligand towards Zn(II) ion. Self-protonation of the Schiff base diminishes its chelation property and prefers stronger interactions with the amino acids / proteins in bacteria.

In our previous work, we studied the bactericidal effect of a mononuclear copper(II)-Schiff base complex containing this same Schiff base [10]. The comparison of MIC values clearly indicates that this zinc complex shows an excellent activity compared to that of the copper(II)-Schiff base complex. Previously, Keypour *et al.* and Das *et al.* synthesized different metal complexes using polydentate Schiff base ligands and studied their antibacterial effect towards different gram positive and gram negative bacteria [56,57]. Their zinc-Schiff base compounds developed good inhibition zone and MIC values against the bacterial species compared to our synthesized zinc-Schiff base complex (Table S4 and Table S5). We also studied the antibacterial effect of Amikacin under identical experimental conditions. Amikacin is a medically recommended antibiotic used for a number of bacterial infections. Truly, this zinc-Schiff base exhibits little activity compared to that of Amikacin (Table S4 and Table S5). Most strikingly, we were able to detect the presence of 1.44% zinc in the chosen zone of inhibition and it was confirmed by energy dispersive X-ray (EDAX) analysis which portrayed the area in a quantitative manner (Fig.S11). This is a rare observation in the study of bactericidal activity and portrays a real promise for the future development of antibacterial agents. Fig. 5 displays the electron microscope scan image which shows the morphological changes in the multiplication of clinical bacillus SP at zone inhibition site and a clear indication of destruction of the bacterial cell membrane.

4. Conclusions

This present study reports the synthesis, crystal structure, supramolecular architecture, bactericidal activity and bio-mimics of 4-MC oxidation of a newly developed zinc-Schiff base complex, $[\text{Zn}(\text{HL})_2\text{Cl}_2]$. Crystal structure analysis reveals that Zn(II) centre adopts a distorted tetrahedral geometry. More captivatingly, the tridentate chelator **actually exists in zwitter ionic form** and behaves a monodentate ligand towards zinc ion. The zinc complex exhibits good bio-mimicking activity towards the oxidation of 4-MC with turnover number, $1.45 \times 10^3 \text{ h}^{-1}$. The electrochemical potential analysis of the zinc complex in presence and absence of 4-MC ensures the production of 4-methyl-*o*-benzosemiquinone ($\text{cat}/\text{sq}^{\cdot-}$) with an active involvement of zinc(II) centre to facilitate the formation of benzo-semiquinone radical. Further, EPR studies confirm the generation of radical species in the course of catalytic oxidation of 4-MC. To the best of our knowledge, our synthetic zinc-Schiff base complex will be the first report to exhibit **4-MC oxidation** activity in scientific literature. The scanning electron **microscopy** images indicate the destruction of bacterial cell membrane and energy dispersive X-ray

spectrum confirmed the existence of 1.44% zinc in the cell membrane. The incorporation of zinc by the bacterial cell will certainly bring some new light in designing future antimicrobial agents of good promise.

Supplementary data

Supplementary crystallographic data are available free of charge from The Director, CCDC, 12 Union Road, Cambridge, CB2 1EZ, UK (fax: +44-1223-336033; E-mail: deposit@ccdc.cam.ac.uk or www: <http://www.ccdc.cam.ac.uk>) upon request, quoting deposition number CCDC 2020846. Experimental information such FT-IR, UV-Vis, ^1H & ^{13}C NMR, ESI mass spectra, rate vs. [substrate] plot, Hirshfeld surface plot, bond distance & bond angle parameters, redox potential data etc are given here.

Acknowledgement

BB thanks SERB, India for financial support under the TEACHERS ASSOCIATESHIP for RESEARCH EXCELLENCE (TAR/000473/2018).

References

- [1] K.L. Haas, K.J. Franz, *Chem. Rev.*, 109 (2009) 4921–4960.
- [2] P.G. Cozzi, *Chem. Soc. Rev.*, 33 (2004) 410-421.
- [3] W. Al Zoubi, Y.G. Ko, *Appl. Organomet. Chem.*, 31 (2017) e3574.
- [4] M. Karar, P. Paul, B. Biswas, T. Majumdar, A. Mallick, *J. Chem. Phys.*, 152 (2020) 075102.
- [5] B. Chowdhury, M. Karar, S. Paul, M. Joshi, A.R. Choudhury, B. Biswas, *Sens. Actuators. B.* 276 (2018) 560-566.
- [6] S. Dutta, J. Mayans, A. Ghosh, *Dalton Trans.*, 49 (2020) 1276-1291.
- [7] M. Karar, S. Paul, B. Biswas, T. Majumdar, A. Mallick, *Dalton Trans.*, 47 (2018) 7059-7069.
- [8] A. Sarkar, A. Chakraborty, T. Chakraborty, S. Purkait, D. Samanta, S. Maity, D. Das, *Inorg. Chem.*, 59 (2020) 9014–9028.
- [9] M. Mondal, S. Ghosh, S. Maity, S. Giri, A. Ghosh, *Inorg. Chem. Front.* 7 (2020) 247-259.

- [10] S. Mahato, N. Meheta, K. Muddukrishnaiah, M. Joshi, P. Ghosh, M. Shit, A.R. Choudhury, B. Biswas, *Appl. Organomet. Chem.*, 34 (2020) e5935.
- [11] P.K. Mudi, N. Bandopadhyay, M. Joshi, M. Shit, S. Paul, A.R. Choudhury, B. Biswas, *Inorg. Chim. Acta*, 505 (2020) 119468.
- [12] A. De, D. Dey, C.K. Pal, S. Paul, B. Biswas, *J. Mol. Struct.* 1195 (2019) 293-301.
- [13] T. Chowdhury, S. Dasgupta, S. Khatua, K. Acharya, D. Das, *ACS Appl. Bio. Mater.*, 3 (2020) 4348–4357.
- [14] S. Das, A. Sahu, M. Joshi, S. Paul, M. Shit, A.R. Choudhury, B. Biswas, *ChemistrySelect*, 3 (2018) 10774-10781.
- [15] W.N. Lipscomb, N. Strater, *Chem. Rev.*, 96 (1996) 2375-2433.
- [16] B.L. Vallee, D.S. Auld, *Acc. Chem. Res.*, 26 (1993) 543-551.
- [17] M. Garai, A. Das, M. Joshi, S. Paul, M. Shit, A.R. Choudhury, B. Biswas, *Polyhedron*, 156 (2018) 223-230.
- [18] D. Dey, G. Kaur, A. Ranjani, L. Gayathri, P. Chakraborty, J. Adhikary, J. Pasan, D. Dhanasekaran, A.R. Choudhury, M.A. Akbarsha, N. Kole, B. Biswas, *Eur. J. Inorg. Chem.*, 2014 (2014) 3350-3358.
- [19] D. Dey, G. Kaur, M. Patra, A.R. Choudhury, N. Kole, B. Biswas, *Inorg. Chim. Acta*, 421 (2014) 335-341.
- [20] S. Pal, B. Chowdhury, M. Patra, M. Maji, B. Biswas, *Spectrochim. Acta, Part A*, 144 (2015) 148–154.
- [21] C.K. Pal, S. Mahato, M. Joshi, S. Paul, A.R. Choudhury, B. Biswas, *Inorg. Chim. Acta*, 506 (2020) 119541.
- [22] A. Erxleben. *Coord. Chem. Rev.* 246 (2003) 203–228.
- [23] P.D. Frischmann, A.J. Gallant, J.H. Chong, M.J. MacLachlan, *Inorg. Chem.*, 47 (2008) 101–112.
- [24] M. Prabhakar, P.S. Zacharias, S.K. Das, *Inorg. Chem.*, 44 (2005) 2585-2587.
- [25] B.F. Abrahams, S.R. Batten, H. Hamit, B.F. Hoskins, R. Robson, *J. Chem. Soc., Chem. Commun.*, (1996) 1313-1314.
- [26] R.S. Joseyphus, M.S. Nair, *Mycobiology*, 36 (2008) 93-98.
- [27] B. Biswas, M. Patra, S. Dutta, M. Ganguly, N. Kole, *J. Chem. Sci.* 125 (2013) 1445-1453.
- [28] R. Yoruk, M.R. Marshall, *J. Food Biochem.*, 27 (2003) 361-422.
- [29] B.B. Mishra, S. Gautam, *Enz. Eng.*, 5 (2016) 141-149.

- [30] M.V. Madinez, J.R. Whitaker, *Trends Food Sci. Tech.*, 6 (1995) 195-200.
- [31] S.M. Shetty, A. Chandrashekar, Y.P. Venkatesh, *Phytochemistry* 72 (2011) 2275-2287.
- [32] J. Borovansky, P. A. Riley, *Melanins and Melanosomes*, Wiley-VCH Verl Co. KGaA, Boschstr, 12, 69469 Weinheim, Germany, (2011).
- [33] J. Reedijk, *Bioinorganic Catalysis*, 1st Ed. Marcel Dekker, New York, (1993).
- [34] S. Mahato, N. Meheta, K. Muddukrishnaiah, M. Joshi, P. Ghosh, M. Shit, A.R. Choudhury, B. Biswas, *Appl. Organomet. Chem.* 34 (2020) e5935.
- [35] CrysAlisPro 1.171.39.35c, (2017) Rigaku Oxford Diffraction, Rigaku Corporation: Tokyo, Japan.
- [36] G.M. Sheldrick, *SHELXT- Integrated space-group and crystal-structure determination. Acta Cryst. A*, 71 (2015) 3-8.
- [37] G.M. Sheldrick, *Acta Cryst. C*, 71 (2015) 3-8.
- [38] O.V. Dolomanov, L.J. Bourhis, R.J. Gildea, J.A.K. Howard, H. Puschmann, *J. Appl. Crystallogr.*, 42 (2009) 339-341.
- [39] M.J. Turner, J.J. McKinnon, S.K. Wolff, D.J. Grimwood, P.R. Spackman, D. Jayatilaka, M.A. Spackman, *Crystal Explorer*, University of Western Australia, <http://hirshfeldsurface.net17> (2017).
- [40] M.A. Spackman, D. Jayatilaka, *Hirshfeld surface analysis. CrystEngCom*, 11 (2009) 19-32.
- [41] S.K. Seth, V.S. Lee, J. Yana, S.M. Zain, A.C. Cunha, V.F. Ferreira, A.K. Jordao, M.C.B.V. de Souza, S.M.S.V. Wardell, J.L. Wardell, E.R.T. Tiekink, *CrystEngComm*, 17 (2015) 2255-2266.
- [42] J. Cabanes, F. Garcia-Canovas, F. Garcia-Carmona, *Biochim. Biophys. Acta, Protein Struct. Mol. Enzymol*, 914 (1987) 190-197.
- [43] (a) T. Zlateva, P.Di Muro, B. Salvato, M. Beltramini. *FEBS Letters.*, 384 (1996) 251-254; (b) C.K. Pal, S. Mahato, H.R. Yadav, M. Shit, A.R. Choudhury, B. Biswas, *Polyhedron*, 174 (2019) 114156; (c) D. Dey, S. Das, H.R. Yadav, A. Ranjani, L. Gyathri, S. Roy, P.S. Guin, D. Dhanasekaran, A.R. Choudhury, M.A. Akbarsha, B. Biswas, *Polyhedron*, 106 (2016) 106-114.
- [44] (a) H.S. Mason, E.W. Peterson, *Biochim. Biophys. Acta*, 111 (1965) 134-146; (b) A. De, M. Garai, H.R. Yadav, A.R. Choudhury, B. Biswas, *Appl. Organomet. Chem.*, 31 (2017) e3551; (c) B. Chowdhury, M. Maji, B. Biswas, *J. Chem. Sci.*, 129 (2017) 1627-1637.
- [45] M. Akagawa, K. Suyama, *Biochem. Biophys. Res. Commun.*, 281 (2001) 193-199.

- [46] E. Faure, C. Falentin-Daudré, T.S. Lanero, C. Vreuls, G. Zocchi, C. Van De Weerd, et al. *Adv. Funct. Mater.*, 22 (2012) 5271-5282.
- [47] A. Daoud, D. Malika, S. Bakari, N. Hfaiedh, K. Mnafigui, A. Kadri, N. Gharsallah. *Arab. J. Chem.* (2015). doi: 10.1016/j.arabjc.2015.07.014.
- [48] F.M. War Nongkhlaw, S.R. Joshi, *J. Microsc. Ultrastruct.*, 5 (2017) 132–139.
- [49] V. Balamurugan, M.S. Hundal, R. Mukherjee. *Eur. J. Chem.*, 10 (2004) 1683.
- [50] (a) R. Xuan, W. Hu, Z. Yang, R. Xuan. *Acta Cryst. C*, 59 (2003) m112-m114; (b) D. Braga, S. M. Draper, E. Champeil, F. Grepioni, *J. Organomet. Chem.* 573 (1999) 73.
- [51] C.K. Pal, S. Mahato, M. Joshi, S. Paul, A.R. Choudhury, B. Biswas, *Inorg. Chim. Acta*, 506 (2020) 119541.
- [52] M. Fraignier, L. Marques, A. Fleuriet, J. Macheix. *J. Agric. and Food Chem.*, 43 (1995) 2375–2380.
- [53] Y. Jiang, X. Duan, H. Qu, Browning: Enzymatic Browning, *Encyclopedia of Food and Health*, 508-514 (2016), <http://dx.doi.org/10.1016/B978-0-12-384947-2.00090-8>.
- [54] F. Hartl, *Inorg. Chim. Acta*, 232 (1995) 99-108.
- [55] A. De, D. Dey, H.R. Yadav, M. Maji, V. Rane, R.M. Kadam, A.R. Choudhury, B. Biswas, *J. Chem. Sci.*, 128 (2016) 1775-1782.
- [56] H. Keypour, F. Forouzandeh, S. Salehzadeh, F. Hajibabaei, S. Feizi, R. Karamian, N. Ghiasi, R. W. Gable, *Polyhedron* 170 (2019) 584-592.
- [57] M. Das, A. Biswas, B.K. Kundu, M.A.J. Charmier, A. Mukherjee, S.M Mobin, G. Udayabhanu, S. Mukhopadhyay, *Chem. Engg. J.* 357 (2019) 447-457.

Table 1. Crystallographic data and structure refinement parameters for zinc-Schiff base

Parameters	1
Empirical formula	$C_{28}H_{26}Cl_2N_2O_4Zn$
Formula weight	590.78
Temperature (K)	298
Crystal system	Triclinic
Space group	<i>P</i> -1
a (Å)	9.2904(4)
b (Å)	10.6979(4)
c (Å)	14.9283(4)
α	94.357(3)
β	97.159(3)
γ	114.451(4)
Volume (Å ³)	1326.67(10)
<i>Z</i>	2
ρ (gcm ⁻³)	1.479
μ (mm ⁻¹)	1.164
F (000)	608
R_{int}	0.083
θ ranges (°)	2.4-32.9
Number of unique reflections	9032
Total number of reflections	24064
Final R indices (R_1 and wR_2)	0.0603, 0.1919
Largest peak and hole (eÅ ⁻³)	0.67, -0.60

Table 2. Bond angles and bond distances value of zinc-Schiff base complex

Bond distances (Å)			
Zn1-O2	1.981(3)	Zn1-Cl1	2.2344(15)
Zn1-O3	1.979(3)	Zn1-Cl2	2.2369(15)
Bond angles (°)			
Cl1-Zn1-Cl2	124.59(5)	Cl2-Zn1-O2	103.97(10)
Cl1-Zn1-O2	104.69(9)	Cl2-Zn1-O3	103.73(9)
Cl1-Zn1-O3	104.42(10)	O2-Zn1-O3	116.31(12)

Table 3. Comparison of K_M values for catalytic oxidation of 4-MC in natural sources and by zinc-Schiff base complex (4-Methylcatechol = 4-MC)

Source	Substrate with higher affinity	K_m (mM)	Optimum pH	Optimum Temperature (°C)	References
Apple (cv.Amasya)	4-MC Catechol	3.1 34.0	7	15	[53]
Apricot	4-MC		5–5.5	25	[52]
Artichoke	4-MC Catechol	10.2 12.4	6	25	[53]
Banana (cv.Anamur)	Catechol	8.5	7	30	[53]
Cherry	4-MC		4.5		[52]
Cucumber	Catechol		7		[53]
Eggplant	4-MC		5–6.5		[53]
Litchi	4-MC	10	7.4	70	[53]
Longan	4-MC		6.5	35	[53]
Olive	4-MC		5.5–7.5		[53]
Peach	4-MC		5		[52]
Plum	4-MC		4–5.5		[52]
[Zn(HL) ₂ Cl ₂]	4-MC	1.38×10^{-3}	5.5	27	This work

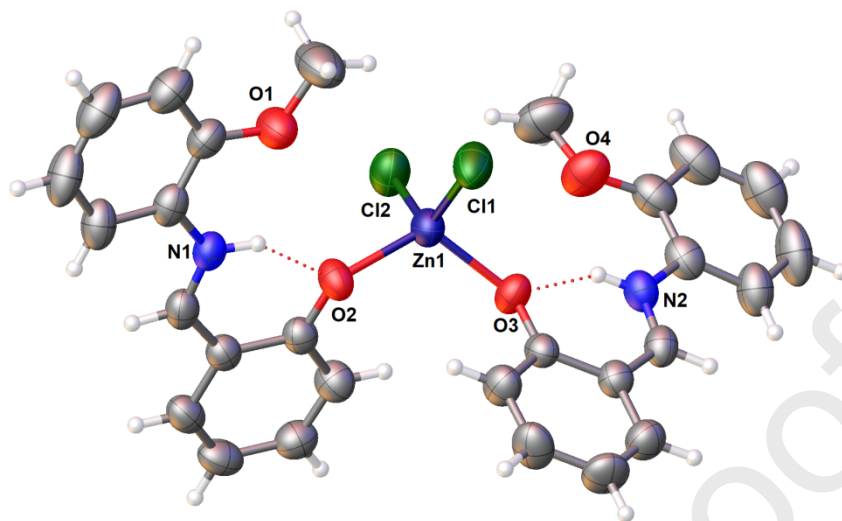


Figure 1. X-ray structure of the zinc-Schiff base complex with 30% ellipsoid probability

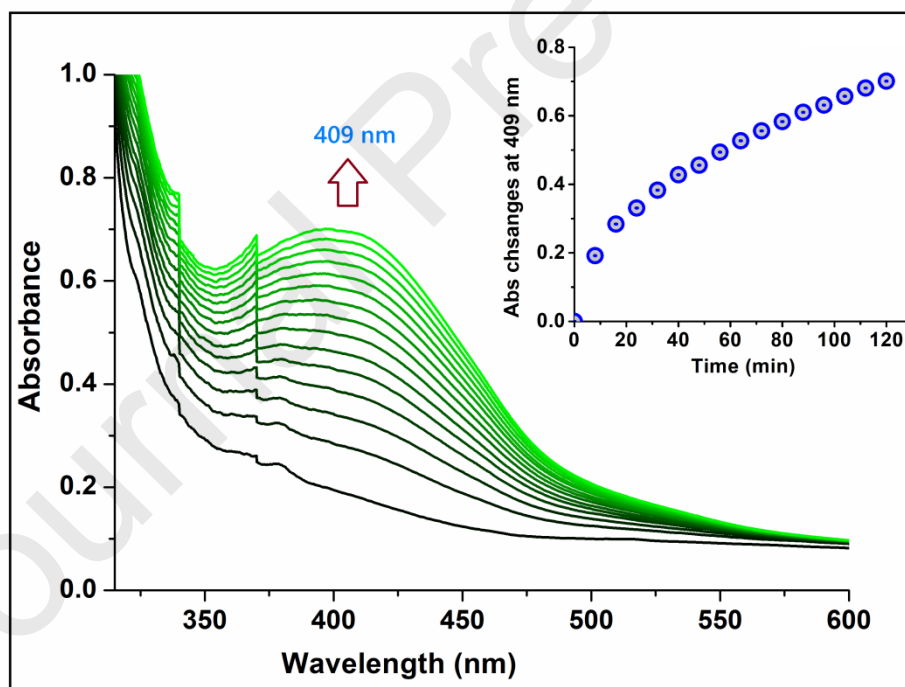


Figure 2. Rise of new electronic band at 409 nm after treatment of zinc complex to 4-MC in MeOH with a time interval of 8 mins. Inset: Time vs Absorbance plot at defined wavelength

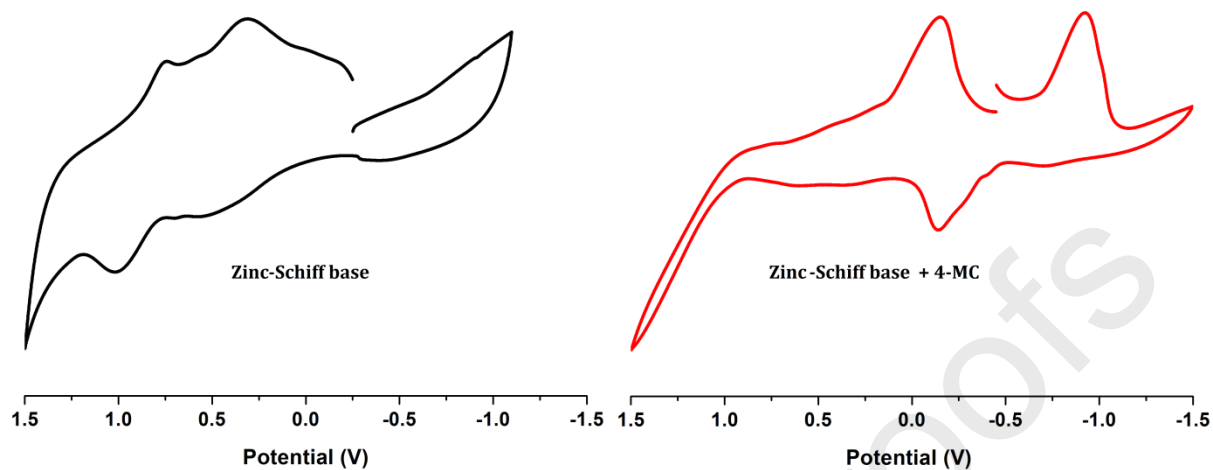


Figure 3. Left: Cyclic voltammogram of the zinc complex in anhydrous DCM medium; **Right:** Cyclic voltammogram of zinc complex in presence of 4-MC under molecular oxygen atmosphere in anhydrous DCM in CH_2Cl_2 (0.20 M $[\text{N}(\text{n-Bu})_4]\text{PF}_6$) at 295 K.

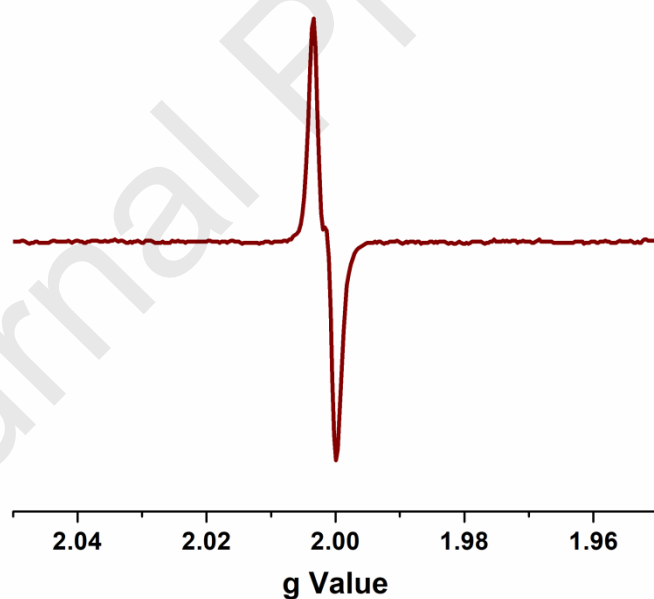


Figure 4. X-band EPR spectrum of 4-MC in presence zinc complex after 10 mins.

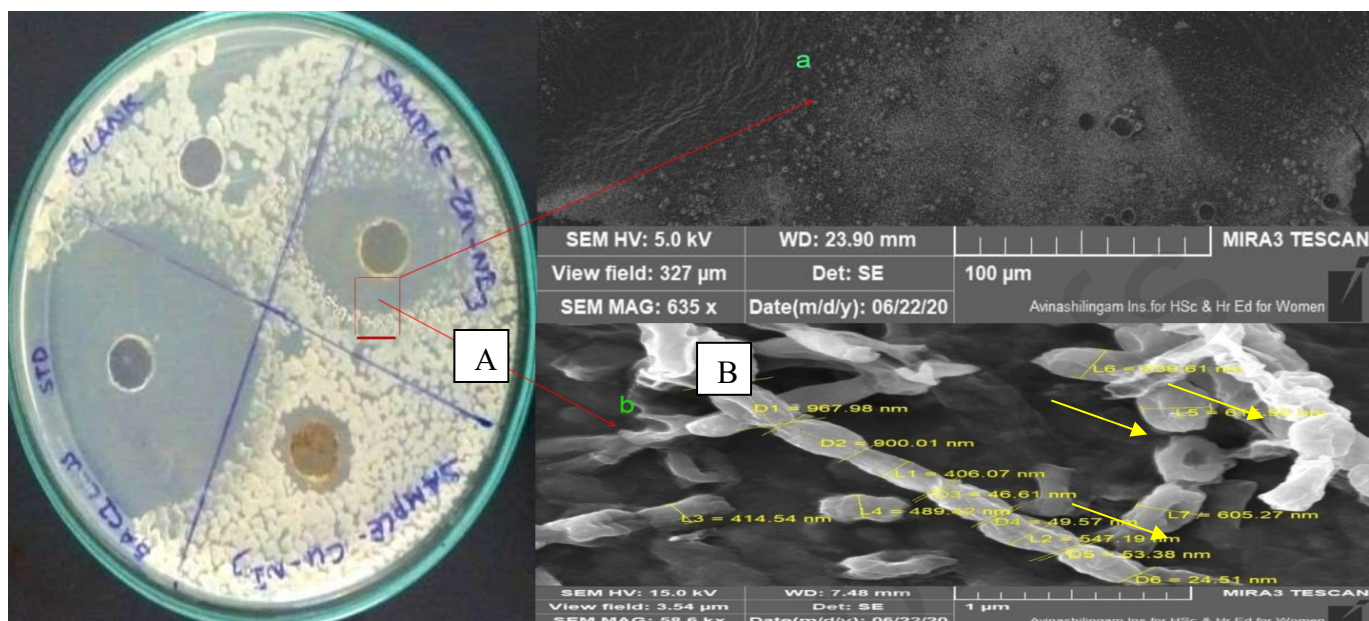


Figure 5. Electron microscope scans showing morphological changes in pathogenic bacteria. A: Zinc complex induced destruction of the bacterial cell membrane (MIC) and B: morphological change of bacterial cell (MBC)

Shreya Mahato: Conceptualization, Formal analysis, Methodology, Investigation; **Nishith Meheta:** Formal analysis, Visualization; **K Muddukrishnaiah:** Solution preparation and study for antimicrobial activity; **Mayank Joshi:** Data analysis; **Madhusudan Shit:** Electrochemical analysis; **Angshuman Roy Choudhury:** X-ray structure analysis; **Bhaskar Biswas:** Writing-Reviewing and Editing, Supervision.

Synthesis, Structure, Polyphenol Oxidase Mimicking and Bactericidal Activity of a Zinc-Schiff Base

Shreya Mahato,^a Nishith Meheta,^a K Muddukrishnaiah,^b Mayank Joshi,^c Madhusudan Shit,^d Angshuman Roy Choudhury,^c and Bhaskar Biswas^{a,*}

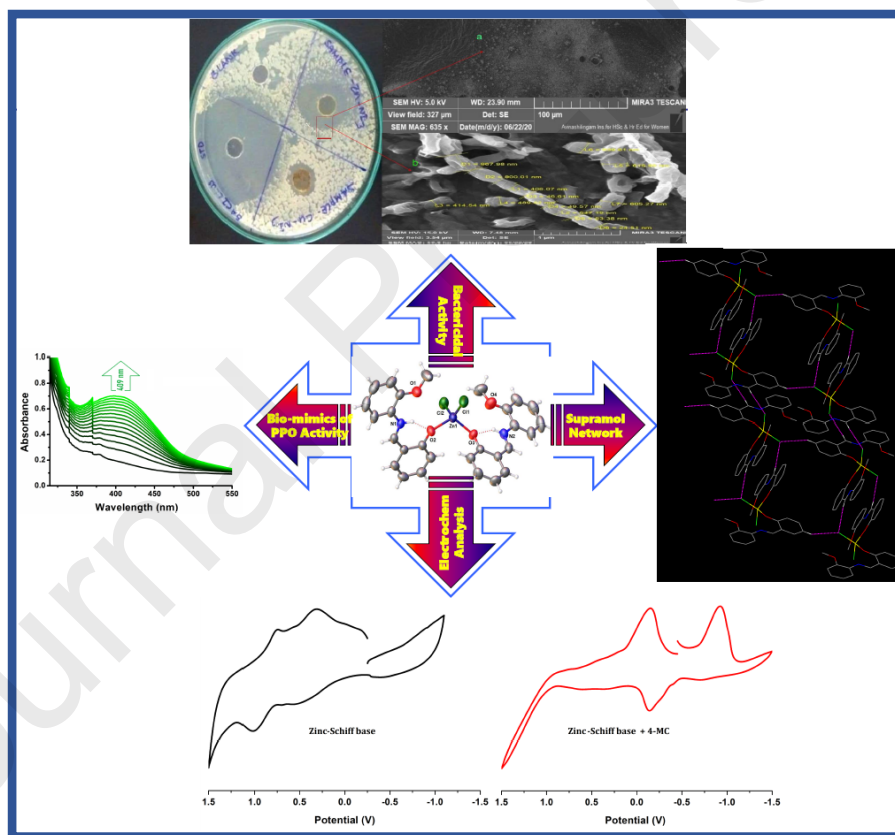
^aDepartment of Chemistry, University of North Bengal, Darjeeling-734013, India

^bDepartment of Pharmaceutical Technology, Anna University, BIT Campus Thiruchirappalli, India

^cDepartment of Chemical Sciences, Indian Institute of Science Education and Research, Mohali, Sector 81, Knowledge City, S. A. S. Nagar, Manauli PO, Mohali, Punjab 140306, India

^dDepartment of Chemistry, Dinabandhu Andrews College, Kolkata 700084, India

This research work demonstrates the synthesis, crystal structure, supramolecular architecture, 4-methylcatechol oxidation and bactericidal activity of a newly designed zinc complex containing a protonated Schiff base of zwitter ion type.



Highlights

- Synthesis and crystal structure of a tetrahedral zinc-Schiff base complex
- Schiff base gets protonated to exhibit monodentate behaviour
- The zinc complex exhibits good efficiency towards the bio-mimetic oxidation of 4-methylcatechol
- Radical driven catalytic activity has been observed.

- Shows good bactericidal activity with 1.44% presence of zinc in cell membrane of bacteria